balt2/zmk-mbc/zmk-mbc/zmk00507/zmk8034-07z | xppws | S=1 | 2/26/07 | 6:51 | 4/Color Figure(s): F1–6 | Art: 3198875 | Input-cip

Myogenesis by Menstrual Blood Cells

Figure 1. Surface marker expression of endometrium-derived cells. (A and B) Morphology of menstrual blood–derived cells, regarded as being PD 1 or 2. Scale bars, 200 μm (A), 100 μm (B). (C and D) Flow cytometric analysis of cell surface markers of EM-E6/E7/hTERT-2 cells (C) and menstrual blood–derived cells (D). (E) Further phenotypic analysis in EM-E6/E7/hTERT-2 cells and menstrual blood–derived cells are summarized. Peak intensity was estimated in comparison with isotype controls. +++, strongly positive (>100 times the isotype control); ++, moderately positive (<100 times but more than 10 times the isotype control), weakly positive (<10 times but more than twice the isotype control), −, negative (less than twice the isotype control).

Surface marker	EM-E6/E7/ hTERT-2 cells	Menstrual blood cells	Surface marker	EM-E6/E7/ hTERT-2 cells	Menstrual blood cells
CD13	+	++	CD55	++	++
CD14	-	-	CD59	++	+++
CD29	++	+++	CD73	+++	+
CD31	-	-	CD90	++	+++
CD34	~	-	CD105	-	++
CD44	+++	+++	c-kit	~	-
CD45	-	-	CD133	-	-
CD50	-	-	HLA-ABC	++	++
CD54	+	++	HLA-DR	-	-

erated and propagated cells express mesenchymal cell-related cell surface markers. Unlike EM-E6/E7/hTERT-2 cells, the menstrual blood–derived adherent cells were positive for CD105. EM-E6/E7/hTERT-2 cells and menstrual blood–derived cells expressed neither hematopoietic lineage markers, such as CD34, nor monocyte-macrophage antigens such as CD14 (a marker for macrophage and dendritic cells), or CD45 (leukocyte common antigen). The lack of expression of CD14, CD34, or CD45 suggests that EM-E6/E7/hTERT-2 cells and the menstrual blood–derived cell culture in the present study is depleted of hematopoietic cells. The cells were also negative for expression of CD31 (PECAM-1), CD50, c-kit, and CD133. The cell population was positive for HLA-ABC, but not for HLA-DR. These results demonstrate that almost all cells derived from endometrium are of mesenchymal origin or stromal origin.

Implanted Endometrium-derived Cells Induce De Novo Myogenesis in Immunodeficient NOG Mice

EM-E6/E7/hTERT-2 cells originate from the endometrial gland and are considered as endometrial progenitor cells or bipotential cells capable of differentiating into both glandular epithelial cells and endometrial stromal cells (Kyo et al., 2003). To determine whether EM-E6/E7/hTERT-2 cells and menstrual blood–derived cells generate complete endometrial structure in vivo, like endometriosis, the cells without any treatment or induction were injected into the right thigh

muscle of immunodeficient NOG mice. PBS without cells was injected into the left thigh muscles as a control. We failed to detect any endometrial structure in the cell-injected site. Immunohistochemical analysis using an antibody specific to human vimentin, an intermediate filament associated with a mesenchymal cell, revealed that the injected EM-E6/E7/hTERT-2 cells (Figure 2, A–F) or menstrual blood–derived cells (Figure 2, G–L) extensively migrated or infiltrated between muscular fibers (Figure 2, arrowheads). To investigate if the donor cells between muscular fibers occur as a result of cell migration, we performed a time-course analysis of implanted cells, as probed by human-specific antibody to vimentin (Supplementary Figure 1). Donor cells at 3 h after implantation are observed at the injection site, which is considered to be due to just injection of cells. Cells at 1–3 wk after implantation are detected between myocytes in the muscle bundle or muscular fascicle as well as in the interstitial tissue, implying that the donor cells between myotubes result from cell migration. Interestingly, some of the vimentin-positive implanted cells exhibited round-shaped structure (Figure 2, D, F, and J, arrows), suggesting that endometrium-derived cells are capable of differentiating into myoblasts/myotubes, and can contribute to skeletal muscle repair in patients suffering from genetic disorders such as DMD, similar to previous reports for marrow stromal cells (Dezawa et al., 2005) and synovial membrane cells (De Bari et al., 2003).
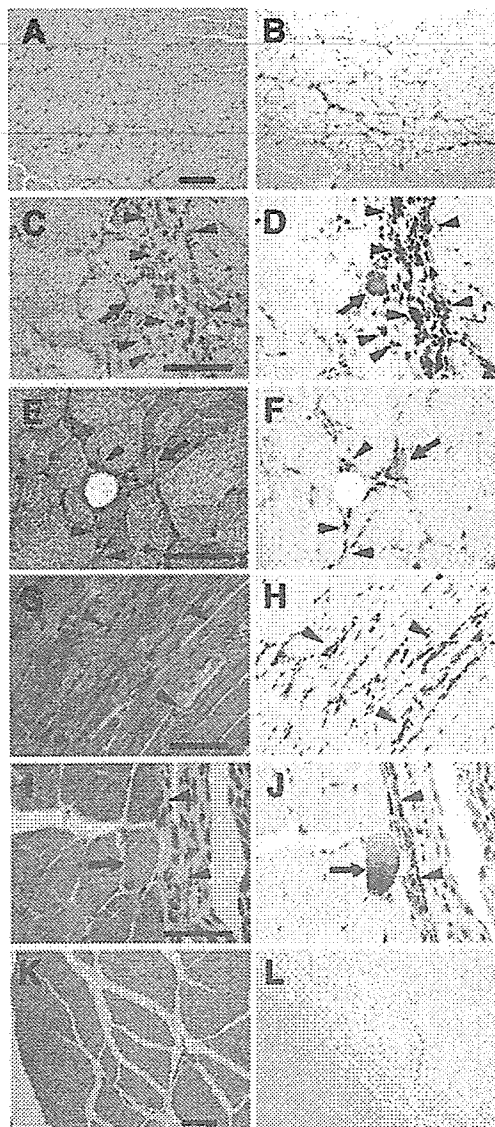
C. Cui et al.

Figure 2. Implantation of endometrium-derived cells-derived cells into the muscle of NOG mice. EM-E6/E7/hTERT-2 cells (A-F) or menstrual blood-derived cells (G-J) cultured in absence of any stimuli were directly injected into the right thigh muscle of NOG mice. Immunohistochemical analysis was performed using antibody that reacts to human vimentin but not to murine vimentin. (A, C, E, G, I, and K) hematoxylin and eosin stain (HE; B, D, F, H, J, and L) immunohistochemistry. Note that vimentin-positive EM-E6/E7/hTERT-2 cells and menstrual blood-derived cells with a spindle morphology (C-J, arrowheads) extensively migrated into muscular bundles at 3 wk after injection, and some of the injected cells exhibited round structure (D, F, and J, arrows). Isotype mouse IgG1 served as a negative control (L). Scale bars, 100 μm (A, B, K, and L), 50 μm (C-F, I, and J), 90 μm (G and H).

Induction of Myogenic Differentiation in Endometrial Progenitor Cells In Vitro

EM-E6/E7/hTERT-2 cells at 2 wk (cultured in the DMEM supplemented with 20% FBS) after exposure to different concentrations (5, 10, and 100 μM) of 5-azacytidine were analyzed by immunostaining using anti-desmin antibody (Figure 3, A-F). The number of desmin-positive cells was

significantly higher in experimental groups with 5 or 10 μM 5-azacytidine than in untreated control groups (p < 0.05). To investigate whether EM-E6/E7/hTERT-2 cells are capable of differentiating into skeletal muscle cells in vitro, the cells were exposed to 5 μM 5-azacytidine for 24 h and then subsequently cultured in the DMEM supplemented with 2% HS (Figure 3, G-J) or serum-free ITS for up to 21 d (Figure 3K). Skeletal myoblastic differentiation of the cells was analyzed by evaluating expression of MyoD, Myf5, desmin, myogenin, MyHC-IIx/d, and dystrophin by RT-PCR. The MyoD, desmin, myogenin, and dystrophin genes were constitutively expressed, but MyHC-IIx/d and Myf5 genes were not. The decline of MyoD was observed in both the 2% HS (Figure 3, G and H) and the serum-free ITS (Figure 3K). The expression of MyHC, as determined by RT-PCR and immunocytochemistry, significantly increased with 2% HS (Figure 3, G-J) and serum-free ITS (Figure 3K). Immunocytochemical analysis indicated that α-sarcomeric actin (Figure 3I) and MyHC (Figure 3J) were detected in the cells incubated with 2% HS for 21 d.

In Vitro Myogenic Differentiation of Menstrual Blood-derived Cells

Menstrual blood-derived cells at 3 wk (cultured in DMEM supplemented with 20% FBS) after exposure to different concentrations (5, 10, and 100 μM) of 5-azacytidine were analyzed by immunostaining using anti-desmin antibody (data not shown). The number of desmin-positive cells was significantly higher in experimental groups with 5 or 10 μM 5-azacytidine than with 100 μM 5-azacytidine; for further in vitro experiments, the menstrual blood-derived cells were exposed to 5 μM 5-azacytidine for 24 h and then subsequently cultured in DMEM supplemented with low serum (2% HS) or serum-free ITS for up to 21 d (Figure 4). Myogenic potential of human menstrual blood-derived cells was analyzed by evaluating the expression of Myf5, MyoD, desmin, myogenin, MyHC-IIx/d, and dystrophin by RT-PCR. MyoD, desmin, and dystrophin genes were constitutively expressed in menstrual blood-derived cells, but MyHC-IIx/d and Myf5 were not (Figure 4A). For cells treated with 2% HS or serum-free ITS, the mRNA level of desmin and myogenin significantly increased after 3 d, and desmin steadily increased until day 21 (Figure 4, C and D). MyHC-IIx/d started to be expressed at a low level at day 21 of induction (Figure 4C). We then analyzed desmin expression by immunocytochemistry. Menstrual blood-derived cells were exposed to 5 μM 5-azacytidine for 24 h and then subsequently cultured in DMEM supplemented with 20% FBS for up to 2 wk. Desmin was readily detected in colonies of the menstrual blood-derived cells (Figure 4B). Western blot analysis indicated that desmin, myogenin, and dystrophin were highly expressed in the cells incubated for 3 wk (Figure 4, E-G). These results suggest that menstrual blood-derived cells are, like the EM-E6/E7/hTERT-2 cells, able to differentiate into skeletal muscle.

Regeneration of Dystrophin by Cell Implantation in the DMD Model mdx-scid Mouse

To investigate whether human EM-E6/E7/hTERT-2 cells and menstrual blood-derived cells can generate muscle tissue in vivo, cells without any treatment or induction were implanted directly into the right thigh muscles of mdx-scid mice (Supplementary Figure 2). The left thigh muscles were injected with PBS as an internal control. After 3 wk, myotubes in the muscle tissues injected with human EM-E6/E7/hTERT-2 cells and menstrual blood-derived cells expressed human dystrophin as a cluster (Figure 5, A, C, and D, EM-
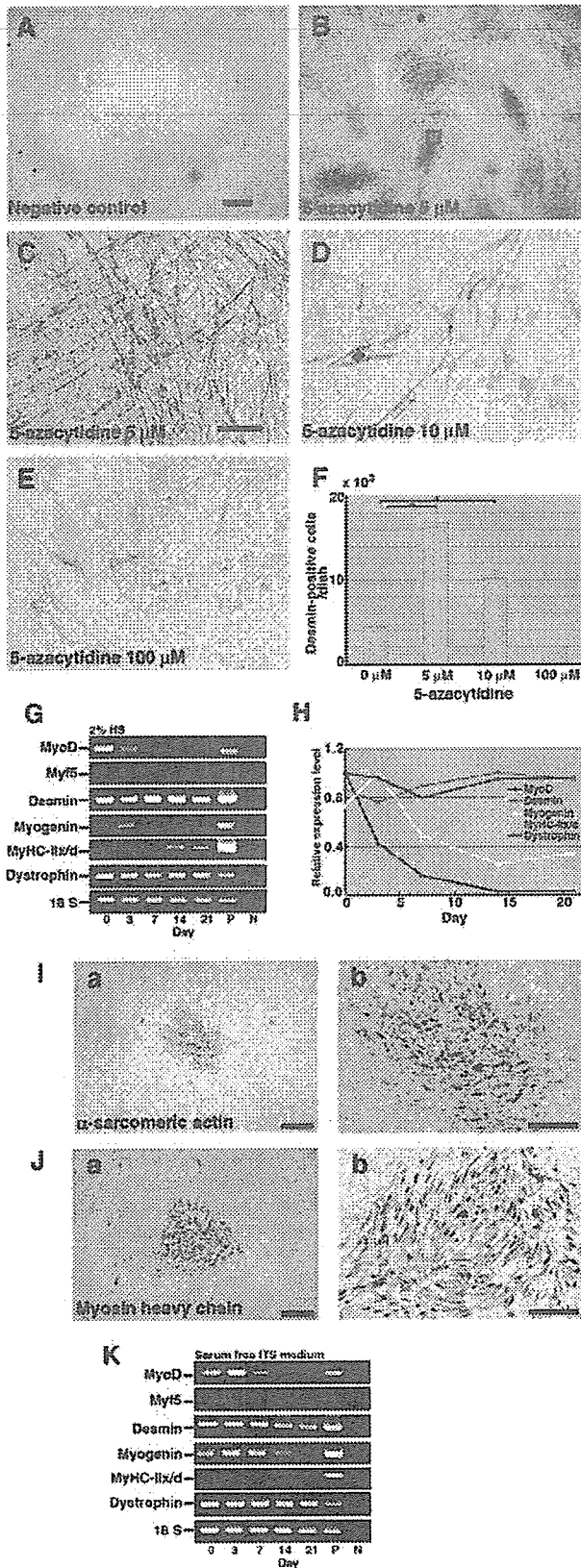
Figure 3. Expression of myogenic-specific genes during myogenic differentiation of EM-E6/E7/hTERT-2 cells. (A–F) Immunocytochemical

E6/E7/hTERT-2 cells, and 5B, menstrual blood–derived cells). Quantification analysis revealed that the percentage of dystrophin-positive myofibers after implantation of menstrual blood–derived cells was high, compared with that after implantation of EM-E6/E7/hTERT-2 cells (Figure 5E). Donor cells with EGFP fluorescence participated in myogenesis 3 wk after implantation (Supplementary Figure 3). EGFP-labeled EM-E6/E7/hTERT-2 cells became positive for human dystrophin (Figure 5C). Dystrophin was not detected in the muscle of mdx-scid mice and NOG mice without cell implantation because the antibody to dystrophin used in this study is human-specific, implying that dystrophin is transcribed from dystrophin genes of human donor cells but not from reversion of dystrophied myocytes in mdx-scid mice.

To determine if dystrophin expression in the donor cells is due to transdifferentiation or fusion, immunohistochemistry with an antibody against human nuclei (Ab-HuNucl) and DAPI stain was performed. If dystrophin expression is explained by fusion, dystrophin-positive myocytes must be demonstrated to have both human and murine nuclei. We examined almost all the 7-μm-thick serial histological sections parallel to the muscular bundle (longitudinal section) of the muscular tissues by confocal microscopy and found that dystrophin-positive myocytes have nuclei derived from both human and murine cells in the longitudinal section of the myocytes (Figure 5D), implying that dystrophin expression is attributed to fusion between murine host myocytes and human donor cells, rather than myogenic differentiation of EM-E6/E7/hTERT-2 cells and menstrual blood–derived cells per se.

Detection of Human Endometrial Cell Contribution to Myotubes in an In Vitro Myogenesis Model

To simulate in vivo phenomena, human endometrial cells were cocultured in vitro with murine C2C12 myoblasts for 2 d under proliferative conditions and then switched to differentiation conditions for an additional 7 d. Figure 6A

analysis of EM-E6/E7/hTERT-2 cells using an antibody to desmin. (A) Omission of only the primary antibody to desmin serves as a negative control. (C) Higher magnification of inset in B. (F) Myogenic differentiation of EM-E6/E7/hTERT-2 cells with exposure to different concentrations (B, 5 μM; C, 5 μM; D, 10 μM, E, 100 μM) of 5-azacytidine. To estimate myogenic differentiation, the number of all the desmin-positive cells was counted for each dish (n = 3). Data were analyzed for statistical significance using ANOVA. EM-E6/E7/hTERT-2 cells were cultured in the DMEM supplemented with 2% HS (G–J; horse serum), and serum-free ITS (K). (G and K) RT-PCR analysis with PCR primers allows amplification of the human MyoD, Myf5, desmin, myogenin, myosin heavy chain type IIx/d (MyHC-IIx/d), and dystrophin cDNA (from top to bottom). RNAs were isolated from EM-E6/E7/hTERT-2 cells at the indicated day after treatment with 5-azacytidine. RNAs from human muscle and H$_2$O served as positive (P) and negative (N) controls. Only the 18S PCR primer used as a positive control reacted with the human and murine cDNA. (H) Time course of MyoD, desmin, myogenin, MyHC-IIx/d, and dystrophin expression in the cells incubated with 2% HS for up to 21 d after 5-azacytidine treatment. Relative mRNA levels were determined using Multi Gauge Ver 2.0 (Fuji Film). The signal intensities of MyoD, desmin, and dystrophin mRNA at day 0, myogenin mRNA at day 3, and MyHC-II/d mRNA at day 21 were regarded as equal to 100%. (I and J) The cells were exposed to 5 μM 5-azacytidine for 24 h and then subsequently cultured in DMEM supplemented with 2% HS for 21 d. α-Sarcomeric actin (I) and skeletal myosin heavy chain (J) was detected by immunocytochemical analysis. Scale bars, 2 mm (A and B), 300 μm (C–E), 900 μm (Ia and Ja), 425 μm (Ib and Jb).
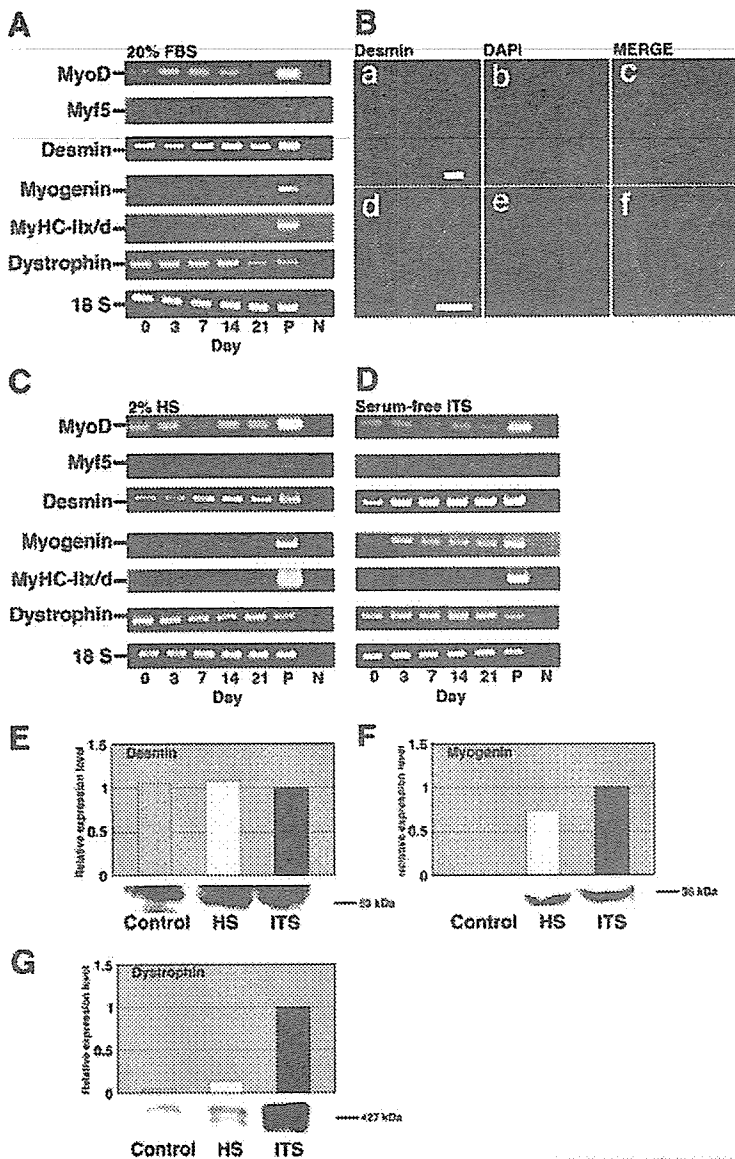
C. Cui *et al.*

Figure 4. Expression of myogenic-specific genes in differentiated menstrual blood–derived cells. Menstrual blood–derived cells were cultured in DMEM supplemented with 20% FBS, 2% HS, or serum-free ITS medium. (A) RT-PCR analysis with PCR primers that allows amplification of the human MyoD, Myf5, desmin, myogenin, MyHC-IIx/d, and dystrophin cDNA (from top to bottom). RNAs were isolated from menstrual blood–derived cells at the indicated day after treatment with 5 μM 5-azacytidine for 24 h. RNAs from human muscle and H_2O served as positive (P) and negative (N) controls. Only the 18S PCR primer used as a positive control reacted with the human and murine cDNA. (B) Immunocytochemical analysis using an antibody to desmin (a–f) was performed on the menstrual blood–derived cells at 2 wk after exposure to 5 μM of 5-azacytidine for 24 h. The desmin-positive cells are shown at higher magnification (d–f). Merge of a and b is shown in c, and merge of d and e is shown in f. The images were obtained with a laser scanning confocal microscope. Scale bars, 200 μm (a–c) and 75 μm (d—f). (C and D) RT-PCR analysis of menstrual blood–derived cells on DMEM supplemented with 2% HS (C) or serum-free ITS medium (D) after exposure to 5 μM 5-azacytidine for 24 h. (E–G) Western blot analysis was performed on the cells cultured in myogenic medium indicated for 21 d. The blot was stained with desmin (E), myogenin (F), and dystrophin (G) antibodies followed by an HRP-conjugated secondary antibody.

provides an example of how human and mouse nuclei in the EGFP-positive myotubes were detected. Multinucleated myotubes were revealed by the presence of specific human dystrophin (Figure 6, B and C) and myosin heavy chain (Figure 6D). Dystrophin was detected in cytoplasm in culture condition (Figure 6, B and C) despite evidence of cell surface localization in vivo. Human dystrophin and human nuclei were unequivocally identified by staining with antibodies to human dystrophin and human nuclei, whereas the numerous mouse nuclei present in this field, as shown by DAPI staining, are negative (Figure 6, B and C).

DISCUSSION

Skeletal muscle has a remarkable regenerative capacity in response to an extensive injury. Resident within adult skeletal muscle is a small population of myogenic precursor cells (or satellite cells) that are capable of multiple rounds of proliferation (estimated at 80–100 doublings), which are

able to reestablish a quiescent pool of myogenic progenitor cells after each discrete regenerative episode (Mauro, 1961; Schultz and McCormick, 1994; Seale and Rudnicki, 2000; Hawke and Garry, 2001). Although muscle regeneration is a highly efficient and reproducible process, it ultimately is exhausted, as observed in senescent skeletal muscle or in patients with muscular dystrophy (Gussoni *et al.*, 1997; Cossu and Mavilio, 2000). In the present study, we investigated the myogenic potential of human endometrial tissue-derived immortalized EM-E6/E7/TERT-2 cells and primary cells derived from human menstrual blood. Human menstrual blood–derived cells proliferated over at least 25 PDs (9 passages) for more than 60 d and stopped dividing before 30 PDs. This cessation of cell division is probably due to replicative senescence or shortening of telomere length. Cell life span of menstrual blood cells is relatively short when compared with human fetal cells (Imai *et al.*, 1994; Terai *et al.*, 2005), and this shorter cell life span may be attributed to shorter telomere length of adult cells (i.e., endometrial stro-
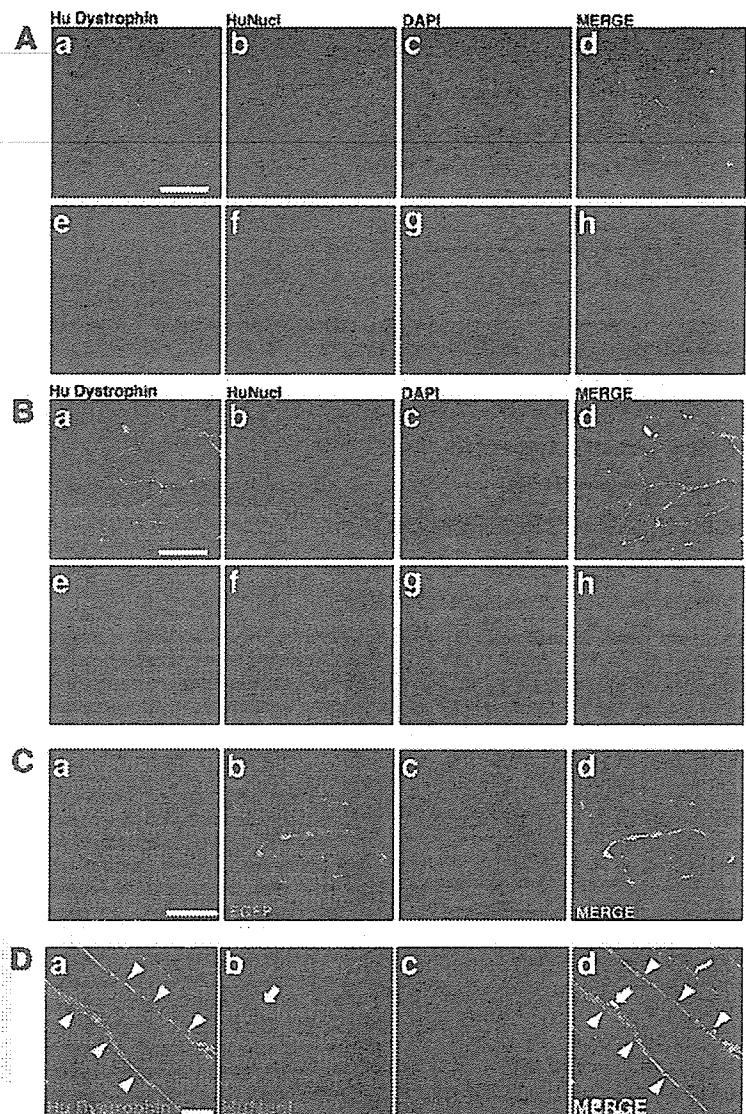
6

Figure 5. Conferral of dystrophin to mdx myocytes by human endometrial cells. (A and B) Immunohistochemistry analysis using an antibody against human dystrophin molecule (green), human nuclei (HuNucl, red), and DAPI staining (blue) on thigh muscle sections of mdx-scid mice after direct injection of EM-E6/E7/hTERT-2 cells (A) or menstrual blood–derived cells (B) without any treatment or induction. (C) EGFP-labeled EM-E6/E7/hTERT-2 cells without any treatment or induction were directly injected into the thigh muscle of mdx-scid mice. Immunohistochemistry revealed the incorporation of implanted cells into newly formed EGFP-positive myofibers, which expressed human dystrophin 3 wk after implantation. (A and B) As a methodological control, the primary antibody to dystrophin was omitted (e and f). (D) Immunohistochemistry analysis using an antibody against human dystrophin molecule (green, arrowheads), human nuclei (HuNucl, red, arrow), and DAPI staining (blue) on thigh muscle sections of mdx-scid mice after direct injection of human EM-E6/E7/hTERT-2 cells without any treatment or induction. (A and B) Merge of a–c is shown in d, and merge of e–g is shown in h. (C and D) Merge of a–c is shown in d. Scale bars, 50 μm (A and B), 20 μm (C and D). (E) Quantitative analysis of human dystrophin-positive myotubes. Menstrual blood–derived cells or EM-E6/E7/hTERT-2 cells without any treatment or induction were directly injected into thigh muscle of mdx-scid mice. The percentage of human dystrophin–positive-myofiber areas was calculated 3 wk after implantation of the EM-E6/E7/hTERT-2 cells or menstrual blood–derived cells. Injection of PBS without cells into mdx-scid myofibers was used as a control.
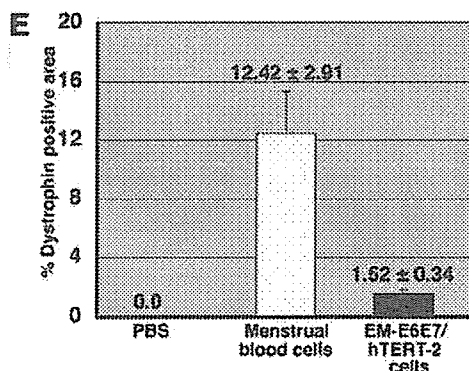
mal cells) at the start of cell cultivation, as is the case with hematopoietic stem cells (Suda et al., 1984).

Menstrual blood–derived cells had a high replicative ability similar to progenitors or stem cells that display a long-term self-renewal capacity and had a much higher growth rate in our experimental conditions than marrow-derived stromal cells (Mori et al., 2005). In addition, the myogenic potential of menstrual blood–derived cells, i.e., a high frequency of desmin-positive cells after induction, is much greater than expected. The higher myogenic differentiation ratio can be explained just by alteration of cell characteristics from epithelial and mesenchymal bipotential cells or heter-
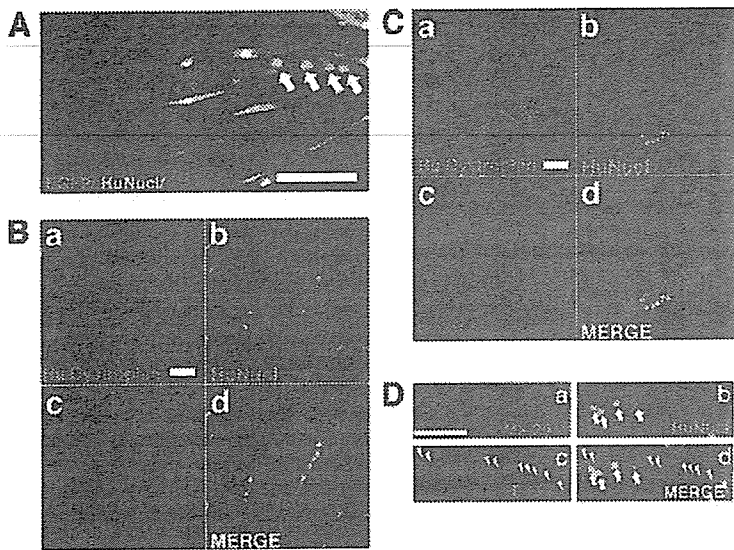
C. Cui et al.

Figure 6. Detection of human endometrial cell contribution to myotubes in an in vitro and in vivo myogenesis model. EGFP-labeled EM-E6/E7/hTERT-2 cells (A) or EM-E6/E7/hTERT-2 cells (B) or menstrual blood–derived cells (C and D) were cocultured with C2C12 myoblasts for 2 d under conditions that favored proliferation. The cultures were then changed to differentiation media for 7 d to induce myogenic fusion. (A) Myotubes were revealed by EGFP (green); human nuclei were detected by antibody specific to human nuclei (HuNucl, red, arrows). (B–D) Myotubes were revealed by specific human dystrophin mAb NCL-DYS3 (B and C, red) or anti-myosin heavy chain mAb MF-20 (D, red). (D) Human nuclei were detected by antibody specific to human nuclei (HuNucl, green, arrows). Total cell nuclei in the culture were stained with DAPI (blue, arrowheads). (B–D) Merge of a–c are shown in d. The cultures were then changed to differentiation media for 7 d to induce myogenic fusion. Scale bars, 100 μm (A–D).

ogeneous populations of cells to cells with the mesenchymal phenotype in our cultivation condition, as determined by cell surface markers (Figure 1, C–E). MyoD-positive cells are present in many fetal chick organs such as brain, lung, intestine, kidney, spleen, heart, and liver (Gerhart et al., 2001), and these cells can differentiate into skeletal muscle in culture. Constitutive expression of MyoD, desmin, and myogenin, all markers for skeletal myogenic differentiation in both immortalized EM-E6/E7/hTERT-2 cells and menstrual blood–derived cells, implies either that most of these cells are myogenic progenitors or that these cells have myogenic potential. Expression of MyoD, one of the basic helix-loop-helix transcription factors that directly regulate myocyte cell specification and differentiation (Edmondson and Olson, 1993), occurs at the early stage of myogenic differentiation, whereas myogenin is expressed later, related to cell fusion and differentiation (Aurade et al., 1994).

Acquisition or recovery of dystrophin expression in dystrophic muscle is attributed to two different mechanisms: 1) myogenic differentiation of implanted or transplanted cells and 2) cell fusion of implanted or transplanted cells with host muscle cells. Recovery of dystrophin-positive cells is explained by muscular differentiation of implanted marrow stromal cells and adipocytes (Dezawa et al., 2005; Rodriguez et al., 2005). In contrast, implantation of normal myoblasts into dystrophin-deficient muscle can create a reservoir of normal myoblasts that are capable of fusing with dystrophic muscle fibers and restoring dystrophin (Mendell et al., 1995; Terada et al., 2002; Wang et al., 2003; Dezawa et al., 2005; Rodriguez et al., 2005). In this study using menstrual blood–derived cells, our findings—that the implantation of immortalized EM-E6/E7/hTERT-2 cells and menstrual blood–derived cells improved the efficiency of muscle regeneration and dystrophin delivery to dystrophic muscle in mice—is explained by both possibilities or the latter possibility alone, because cells expressing human dystrophin had both murine and human nuclei, located in the center and periphery of dystrophic muscular fiber, respectively (Figures 5D, in vivo, and 6, A–D, in vitro).

DMD is a devastating X-linked muscle disease characterized by progressive muscle weakness attributable to a lack of dystrophin expression at the sarcolemma of muscle fibers (Mendell et al., 1995; Rodriguez et al., 2005), and there are no

effective therapeutic approaches for muscular dystrophy at present. Human menstrual blood–derived cells are obtained by a simple, safe, and painless procedure and can be expanded efficiently in vitro. In contrast, isolation of mesenchymal stem cells/mesenchymal cells from other sources, such as bone marrow and adipose tissue, is accompanied by a painful and complicated operation. Efficient fusion systems of our immortalized human EM-E6/E7/hTERT-2 cells and menstrual blood–derived cells with host dystrophic myocytes may contribute substantially to a major advance toward eventual cell-based therapies for muscle injury or chronic muscular disease. Finally, we would like to reemphasize that human menstrual blood–derived cells possess high self-renewal capacity, whereas biopsied myoblasts capable of differentiating into muscular cells are poorly expandable in vitro and rapidly undergo senescence (Cossu and Mavilio, 2000).

ACKNOWLEDGMENTS

REFERENCES

Aurade, F., Pinset, C., Chafey, P., Gros, F., and Montarras, D. (1994). Myf5, MyoD, myogenin and MRF4 myogenic derivatives of the embryonic mesenchymal cell line C3H10T1/2 exhibit the same adult muscle phenotype. Differentiation 55, 185–192.

Bischoff, R. (1994). The satellite cell and muscle regeneration. In: Myology: Basic and Clinical, ed. A. Engel, C. Franzini-Armstrong, and D. A. Fischman, New York: McGraw-Hill, Health Professions Division, 97–118.

Cossu, G., and Mavilio, F. (2000). Myogenic stem cells for the therapy of primary myopathies: wishful thinking or therapeutic perspective? J. Clin. Invest. 105, 1669–1674.

De Bari, C., Dell'Accio, F., Vandenabeele, F., Vermeesch, J. R., Raymackers, J. M., and Luyten, F. P. (2003). Skeletal muscle repair by adult human mesenchymal stem cells from synovial membrane. J. Cell Biol. 160, 909–918.

Dezawa, M., Ishikawa, H., Itokazu, Y., Yoshihara, T., Hoshino, M., Takeda, S., Ide, C., and Nabeshima, Y. (2005). Bone marrow stromal cells generate muscle cells and repair muscle degeneration. Science 309, 314–317.

Edmondson, D. G., and Olson, E. N. (1993). Helix-loop-helix proteins as regulators of muscle-specific transcription. J. Biol. Chem. 268, 755–758.

Ervasti, J. M., and Campbell, K. P. (1991). Membrane organization of the dystrophin-glycoprotein complex. Cell 66, 1121–1131.

Gerhart, J., Bast, B., Neely, C., Iem, S., Amegbe, P., Niewenhuis, R., Miklasz, S., Cheng, P. F., and George-Weinstein, M. (2001). MyoD-positive myoblasts are present in mature fetal organs lacking skeletal muscle. J. Cell Biol. 155, 381–392.

Grounds, M. D., White, J. D., Rosenthal, N., and Bogoyevitch, M. A. (2002). The role of stem cells in skeletal and cardiac muscle repair. J. Histochem. Cytochem. 50, 589–610.

Gussoni, E., Blau, H. M., and Kunkel, L. M. (1997). The fate of individual myoblasts after transplantation into muscles of DMD patients. Nat. Med. 3, 970–977.

Hasty, P., Bradley, A., Morris, J. H., Edmondson, D. G., Venuti, J. M., Olson, E. N., and Klein, W. H. (1993). Muscle deficiency and neonatal death in mice with a targeted mutation in the myogenin gene. Nature 364, 501–506.

Hawke, T. J., and Garry, D. J. (2001). Myogenic satellite cells: physiology to molecular biology. J. Appl. Physiol. 91, 534–551.

Hoffman, E. P., Brown, R. H., Jr., and Kunkel, L. M. (1987). Dystrophin: the protein product of the Duchenne muscular dystrophy locus. Cell 51, 919–928.

Imai, S., Fujino, T., Nishibayashi, S., Manabe, T., and Takano, T. (1994). Immortalization-susceptible elements and their binding factors mediate rejuvenation of regulation of the type I collagenase gene in simian virus 40 large T antigen-transformed immortal human fibroblasts. Mol. Cell. Biol. 14, 7182–7194.

Kyo, S., Nakamura, M., Kiyono, T., Maida, Y., Kanaya, T., Tanaka, M., Yatabe, N., and Inoue, M. (2003). Successful immortalization of endometrial glandular cells with normal structural and functional characteristics. Am. J. Pathol. 163, 2259–2269.

Mauro, A. (1961). Satellite cell of skeletal muscle fibers. J. Biophys. Biochem. Cytol. 9, 493–495.

Mendell, J. R. et al. (1995). Myoblast transfer in the treatment of Duchenne's muscular dystrophy. N. Engl. J. Med. 333, 832–838.

Miyoshi, H., Blomer, U., Takahashi, M., Gage, F. H., and Verma, I. M. (1998). Development of a self-inactivating lentivirus vector. J. Virol. 72, 8150–8157.

Miyoshi, H., Takahashi, M., Gage, F. H., and Verma, I. M. (1997). Stable and efficient gene transfer into the retina using an HIV-based lentiviral vector. Proc. Natl. Acad. Sci. USA 94, 10319–10323.

Mori, T. et al. (2005). Combination of hTERT and bmi-1, E6, or E7 induces prolongation of the life span of bone marrow stromal cells from an elderly donor without affecting their neurogenic potential. Mol. Cell. Biol. 25, 5183–5195.

Nabeshima, Y., Hanaoka, K., Hayasaka, M., Esumi, E., Li, S., Nonaka, I., and Nabeshima, Y. (1993). Myogenin gene disruption results in perinatal lethality because of severe muscle defect. Nature 364, 532–535.

Rodriguez, A. M. et al. (2005). Transplantation of a multipotent cell population from human adipose tissue induces dystrophin expression in the immuno-competent mdx mouse. J. Exp. Med. 201, 1397–1405.

Rudnicki, M. A., Schnegelsberg, P. N., Stead, R. H., Braun, T., Arnold, H. H., and Jaenisch, R. (1993). MyoD or Myf-5 is required for the formation of skeletal muscle. Cell 75, 1351–1359.

Sabourin, L. A., and Rudnicki, M. A. (2000). The molecular regulation of myogenesis. Clin. Genet. 57, 16–25.

Schultz, E., and McCormick, K. M. (1994). Skeletal muscle satellite cells. Rev. Physiol. Biochem. Pharmacol. 123, 213–257.

Seale, P., and Rudnicki, M. A. (2000). A new look at the origin, function, and "stem-cell" status of muscle satellite cells. Dev. Biol. 218, 115–124.

Sicinski, P., Geng, Y., Ryder-Cook, A. S., Barnard, E. A., Darlison, M. G., and Barnard, P. J. (1989). The molecular basis of muscular dystrophy in the mdx mouse: a point mutation. Science 244, 1578–1580.

Suda, J., Suda, T., and Ogawa, M. (1984). Analysis of differentiation of mouse hemopoietic stem cells in culture by sequential replating of paired progenitors. Blood 64, 393–399.

Terada, N., Hamazaki, T., Oka, M., Hoki, M., Mastalerz, D. M., Nakano, Y., Meyer, E. M., Morel, L., Petersen, B. E., and Scott, E. W. (2002). Bone marrow cells adopt the phenotype of other cells by spontaneous cell fusion. Nature 416, 542–545.

Terai, M., Uyama, T., Sugiki, T., Li, X. K., Umezawa, A., and Kiyono, T. (2005). Immortalization of human fetal cells: the life span of umbilical cord blood-derived cells can be prolonged without manipulating p16INK4a/RB braking pathway. Mol. Biol. Cell 16, 1491–1499.

Wang, X., Willenbring, H., Akkari, Y., Torimaru, Y., Foster, M., Al-Dhalimy, M., Lagasse, E., Finegold, M., Olson, S., and Grompe, M. (2003). Cell fusion is the principal source of bone-marrow-derived hepatocytes. Nature 422, 897–901.

JCB-06-0405(21125)

Hyaline Cartilage Formation and Enchondral Ossification Modeled With KUM5 and OP9 Chondroblasts

Tadashi Sugiki,[1,2] Taro Uyama,[1] Masashi Toyoda,[1] Hideo Morioka,[2] Shoen Kume,[3] Kenji Miyado,[1] Kenji Matsumoto,[4] Hirohisa Saito,[4] Noriyuki Tsumaki,[5] Yoriko Takahashi,[6] Yoshiaki Toyama,[2] and Akihiro Umezawa[1]*

[1]Department of Reproductive Biology and Pathology, National Institute for Child and Health Development, Tokyo 157-8535, Japan
[2]Department of Orthopaedic Surgery, Keio University School of Medicine, Tokyo 160-8582, Japan
[3]Division of Stem Cell Biology, Department of Regeneration Medicine, Institute of Molecular Embryology and Genetics, Kumamoto University, Kuhonji, Kumamoto 862-0976, Japan
[4]Department of Allergy & Immunology, National Research Institute for Child Health and Development, Tokyo, Japan
[5]Department of Orthopaedics, Osaka University Graduate School of Medicine, 2-2 Yamadaoka, Suita, Osaka 565-0871, Japan
[6]Mitsui Knowledge Industry, Co, Ltd, Harmony Tower 21st Floor, 1-32-2 Honcho, Nakano-ku, Tokyo 164-8721, Japan

Abstract   What is it that defines a bone marrow-derived chondrocyte? We attempted to identify marrow-derived cells with chondrogenic nature and immortality without transformation, defining "immortality" simply as indefinite cell division. KUM5 mesenchymal cells, a marrow stromal cell line, generated hyaline cartilage in vivo and exhibited enchondral ossification at a later stage after implantation. Selection of KUM5 chondroblasts based on the activity of the chondrocyte-specific cis-regulatory element of the collagen α2(XI) gene resulted in enhancement of their chondrogenic nature. Gene chip analysis revealed that OP9 cells, another marrow stromal cell line, derived from macrophage colony-stimulating factor-deficient osteopetrotic mice and also known to be niche-constituting cells for hematopoietic stem cells expressed chondrocyte-specific or -associated genes such as type II collagen α1, Sox9, and cartilage oligomeric matrix protein at an extremely high level, as did KUM5 cells. After cultured OP9 micromasses exposed to TGF-β3 and BMP2 were implanted in mice, they produced abundant metachromatic matrix with the toluidine blue stain and formed type II collagen-positive hyaline cartilage within 2 weeks in vivo. Hierarchical clustering and principal component analysis based on microarray data of the expression of cell surface markers and cell-type-specific genes resulted in grouping of KUM5 and OP9 cells into the same subcategory of "chondroblast," that is, a distinct cell type group. We here show that these two cell lines exhibit the unique characteristics of hyaline cartilage formation and enchondral ossification in vitro and in vivo. J. Cell. Biochem. 9999: 1–15, 2006.   © 2006 Wiley-Liss, Inc.

Key words: Hyaline cartilage; chondroblasts; enchondral[Q2] ossification; bioinformatics; gene chip

The concept of regenerative medicine refers to the cell-mediated restoration of damaged or diseased tissue, and practically, regeneration of bone and cartilage may be one of the most accessible approaches. Candidate cell sources for regeneration of tissue include embryonic stem cells, fetal cells, or adult cells such as marrow stromal cells [Bianco and Robey, 2000], each of which has both benefits and drawbacks. Multipotent mesenchymal stem cells proliferate extensively, and to maintain the ability to differentiate into multiple cell types such as osteoblasts, chondrocytes, cardiomyocytes, adipocytes, and myoblasts in vitro [Umezawa et al., 1992; Pittenger et al., 1999; Bianco and Robey, 2000]. Marrow-derived stromal cells are also able to generate cardiomyocytes and endothelial cells [Makino et al., 1999], neuronal cells [Kohyama et al., 2001], and adipocytes [Umezawa et al., 1991]. Thus, marrow stromal cells are expected to be a good source of cell therapy in addition to embryonic stem cells and fetal cells [Pittenger et al., 1999].

In adults, chondrocytes maintain the extracellular matrix that gives cartilage its unique mechanical properties. Chondrocytes are long-lived and the development of new cells that are capable of producing cartilage de novo (i.e., chondroblasts) is not a normal part of adult cartilage physiology. A better understanding of the molecular mechanisms that regulate postnatal chondroblast differentiation would have a high impact on the design of strategies for cartilage repair. Cultures are commonly made from suspensions of cells dissociated from cartilage. Cartilage-derived cells in primary cultures can be removed from the culture dish and made to proliferate to form a large number of so-called secondary cultures: in this way, these cells may be repeatedly subcultured for weeks or months. Such cells often display many of the differentiated properties appropriate to their origin: the phenotype of the differentiated chondrocyte is characterized by the synthesis, deposition, and maintenance of cartilage-specific extracellular matrix molecules, including type II collagen and aggrecan [Archer et al., 1990; Hauselmann et al., 1994; Reginato et al., 1994]. The phenotype of differentiated chondrocytes is unstable in culture and is rapidly lost during serial monolayer subculturing [Benya and Shaffer, 1982; Lefebvre et al., 1990; Bonaventure et al., 1994]. This process is referred to as "dedifferentiation" and is a major impediment to the use of mass cell populations for cell therapy or tissue engineering of damaged cartilage. However, when cultured three-dimensionally in a scaffold such as agarose, collagen, or alginate, redifferentiated chondrocytes start to reexpress the chondrocytic differentiation phenotype.

This study was undertaken to obtain bone marrow-derived chondroblastic cell lines that retain critical in vivo cell functions. Previous studies showed that it was possible to obtain lines of bone marrow-derived mesenchymal stem cells, mammary gland epithelial cells, skin keratinocytes, and pigmented epithelial cells that retained critical in vivo cell functions. By implanting cells into immunodeficient mice, we identified a newly isolated KUM5 chondroblastic cell line capable of in vivo hyaline-type chondrogenesis and serendipitously found that OP9 cells derived from osteopetrotic mice and also known as a niche-constituting cells for hematopoietic stem cells had chondrogenic potential.

MATERIALS AND METHODS

Cell Culture and Chondrogenic Differentiation

The cells were cultured in the growth medium (GM): Dulbecco's modified Eagle's medium (DMEM) with high glucose supplemented with 10% fetal bovine serum for KUM5 cells; α-MEM supplemented with 10% serum (BIOWEST, lot number: S03400S1820) for OP9 cells. For chondrogenic induction of pellet culture [Johnstone et al., 1998], both KUM5 and OP9 cells were cultured in the chondrogenic medium (CM): DMEM-high glucose containing 0.1 μM dexamethasone, 1 mM sodium pyruvate, 0.17 mM ascorbic acid-2-phosphate, 0.35 mM proline, 6.25 μg/ml bovine insulin, 6.25 μg/ml transferrin, 6.25 μg/ml selenous acid, 5.33 μg/ml linoleic acid, and 1.25 mg/ml BSA (BioWhittaker). In the chondrogenic differentiation, the combination of one or several growth factors was added to the CM: TGF-β3 10 ng/ml, BMP2 50 ng/ml, BMP4 50 ng/ml, BMP6 50 ng/ml, BMP7 50 ng/ml, PDGF 50 ng/ml, hyaluronic acid 250 ng/ml. The cells and the pellets were maintained at 37°C with 5% CO_2.

Scanning Electron Microscopy (SEM) and Transmission Electron Microscopy (TEM)

The pelleted micromasses were examined by SEM and TEM. The micromasses were coated

with gold using a Sputter Coater (Sanyu Denshi Co., Tokyo, Japan) for SEM. The gas pressure was set at 50 mtorr, the current was 5 mA, and the coating time was 180 s. The samples were examined with a scanning electron microscope (JSM-6400Fs; JEOL, Ltd., Tokyo, Japan) operated at a voltage of 3 kV. For TEM, the micromasses and cell implants were initially fixed in PBS containing 2.5% glutaraldehyde for 24 h, and were embedded in epoxy resin. Ultrathin sections were double stained with uranyl acetate and lead citrate and were viewed under a JEM-1200EX transmission electron microscope (JEOL, Ltd.).

Flow Cytometric Analysis

Flow cytometric analysis was performed as previously described [Ochi et al., 2003; Mori et al., 2005; Terai et al., 2005].

Preparation and Transfection of Plasmid

The Venus gene (gift from Miyawaki) was obtained by BamHI and NotI digestion of Venus/pCS2 [Nagai et al., 2002]. The Venus gene was then cloned between the BamHI and NotI sites of pBluescriptII SK (−), excised by SalI and NotI digestion, and inserted between the XhoI and NotI sites of the p742-LacZ plasmid [Tsumaki et al., 1996], from which the LacZ gene was excised by XhoI and NotI digestion. This was named p742-Venus-Int plasmid. Transfection was performed using LipofectAmine 2000 (Invitrogen) according to the manufacturer's instructions.

Isolation of KUM5 Chondroblast

Cells were transfected with p742-Venus-Int plasmid and were cultured for 72 h. Venus-positive cells were sorted using the cell sorter (EPICS ALTRA, Beckman Courter).

In Vivo Cell Implantation Assay

To determine the ability of cultured cells to differentiate in vivo, freshly scraped cells (2–3 × 10⁷ cells) were subcutaneously inoculated into Balb/c nu/nu mice (Sankyo Laboratory, Hamamatsu, Japan) as previously described [Umezawa et al., 1992]. Animals were sacrificed by cervical dislocation between 1 and 8 weeks after inoculation. The subcutaneous specimens were dissected at various times after implantation and fixed and decalcified for 1 week in 10% EDTA (pH 8.0) solution. After dehydration in ascending concentrations of ethanol and xylene,

the implants were embedded in paraffin. The paraffin sections were then deparaffinized, hydrated, and stained with hematoxylin and eosin, alcian blue, or toluidine blue. Paraffin sections were immunohistochemically stained with anti-type II collagen antibodies (Daiichi Fine Chemical Co., Ltd., Tokyo, Japan, Product No. F-57).

All animals received humane care in compliance with the "Principles of Laboratory Animal Care" formulated by the National Society for Medical Research and the "Guide for the Care and Use of Laboratory Animals" prepared by the Institute of Laboratory Animal Resources and published by the US National Institutes of Health (NIH Publication No. 86–23, revised 1985). The operation protocols were accepted by the Laboratory Animal Care and Use Committee of the Research Institute for Child and Health Development (2003–002).

Gene Chip Expression Analysis

Mouse-genome-wide gene expression was examined with the Mouse Genome MOE430A Probe array (GeneChip, Affymetrix), which contains the oligonucleotide probe set for approximately 23,000 full-length genes and expressed sequence tags (ESTs), according to the manufacturer's protocol (Expression Analysis Technical Manual and GeneChip small sample target labeling Assay Version 2 technical note. http://www.affymetrix.com/support/technical/index.affx). Total RNA was isolated with an RNeasy mini-kit (Qiagen, Chatsworth, CA). Double-stranded cDNA was synthesized, and the cDNA was subjected to in vitro transcription in the presence of biotinylated nucleoside triphosphates. The biotinylated cRNA was hybridized with a probe array for 16 h at 45°C, and the hybridized biotinylated cRNA was stained with streptavidin-PE and scanned with a Hewlett–Packard Gene Array Scanner. The fluorescence intensity of each probe was quantified by using the GeneChip Analysis Suite 5.0 computer program (Affymetrix). The expression level of a single mRNA was determined as the average fluorescence intensity among the intensities obtained with 11 paired (perfect matched and single nucleotide-mismatched) probes consisting of 25-mer oligonucleotides. If the intensities of mismatched probes was very high, gene expression was judged to be absent (A), even if high average fluorescence was obtained with the GeneChip Analysis Suite 5.0 program. The

level of gene expression was determined with the GeneChip software as the average difference (AD). Specific AD levels were then calculated as percentages of the mean AD level of six probe sets for housekeeping genes (β-actin and GAPDH). Further data analysis was performed with the Genespring software version 5 (Silicon Genetics, San Carlos, CA). To normalize the staining intensity variations among chips, the AD values for all genes on a given chip were divided by the median of all measurements on that chip. To eliminate changes within the range of background noise and to select the most differentially expressed genes, data were used only if the raw data values were less than 100 AD and gene expression was judged to be present by the Affymetrix data analysis.

Hierarchical Clustering and Principal Component Analysis

To analyze the gene expression data in an unsupervised manner by gene chip array, we used agglomerative hierarchical clustering and principal component analysis (PCA) (http://lgsun.grc.nia.nih.gov/ANOVA/). The hierarchical clustering techniques classify data by similarity and there results are represented by dendrogram. PCA is a multivariate analysis technique which finds major pattern in data variability. Hierarchical clustering and PCA were performed to group mesenchymal cells obtained from bone marrow into subcategories. Expression data of 244 cell surface marker genes (Supplementary Table I), 34 fat-associated genes (Supplementary Table II), 36 cartilage-associated genes (Supplementary Table III) dotted onto the gene chip were used for analysis.

RESULTS

Pelleted Micromass Culture of KUM5 Cells

KUM5 cells, one of the cloned lines of cells, were found to exhibit chondrogenesis in vivo within 4 weeks after direct injection. This possible chondrogenic cell line was subcloned by the limiting dilution method to obtain a cell line capable of forming elastic, fibrous or hyaline cartilage. When cultured in monolayer, KUM5 cells had a fibroblast-like morphology, and their doubling time was approximately 29.7 h. After reaching confluence, the cells had larger nucleus and cytoplasm, and generated so-called "chondrogenic nodules." We per-

formed the micromass culture of KUM5 cells in the GM or the CM, and continued the pelleted micromass culture for up to 10 weeks (Fig. 1A). The cells were equally embedded in the extracellular matrix, and the extracellular matrix of the KUM5 pellet culture did not show metachromasia with toluidine blue staining in the GM and the CM. Since transforming growth factor (TGF)-β and bone morphogeneic protein (BMP) are involved in chodrogenesis and osteogenesis [Fujii et al., 1999; Maeda et al., 2004], we used TGF-β3 and BMPs on KUM5 culture. Exposure of the cells to TGF-β3 augmented the metachromatic toluidine blue staining in the KUM5-micromass (Fig. 1A,B). BMP2 dramatically enhanced this TGF-β3-induced differentiation, that is, caused stronger metachromatic staining and enlarged metachromatic area. To determine the effect of other cytokines on the TGF-β3-induced chondrogenic differentiation, we added BMP4, BMP6, BMP7, PDGF, or hyaluronic acid to the CM supplemented with TGF-β3. BMP4, BMP6, and BMP7 enhanced the TGF-β3-induced chondrogenic differentiation in a manner similar to BMP2 (Fig. 1C,D). With exposure to BMP2, the number of the postmitotic daughter cells in the cell nest increased, matrix became more abundant, and hypertrophic chondrocytes became larger at higher magnification (Fig. 1E). In contrast, PDGF inhibited the TGF-β3 and BMP4-induced differentiation, as determined by toluidine blue staining (Fig. 1Ce,De). To confirm the chondrogenetic differentiation histologically, we examined the ultrastructural analysis of the cartilaginous micromasses. Extracellular matrix was abundantly deposited over KUM5 cells, or the surface of the generated micromass. The cells covering the micromass showed a flattened shape (Fig. 3A,B). The KUM5 chondrocytes inside the micromass showed an oval or round structure, had cellular processes, and were embedded in the hypertrophic chondrocytes. Abundant rough endoplasmic reticulum and a small number of mitochondria were observed in the KUM5 chondrocytes (Fig. 3C).

Gene Chip Analysis of the KUM5 and OP9 Chondroblasts

To clarify the specific gene expression profile of marrow stromal cells, we compared the expression levels of approximately 23,000 genes in the KUM5, 9-15c, KUSA-O, KUSA-A1, H-1/A, and OP9 cells [Umezawa et al., 1992; Nakano
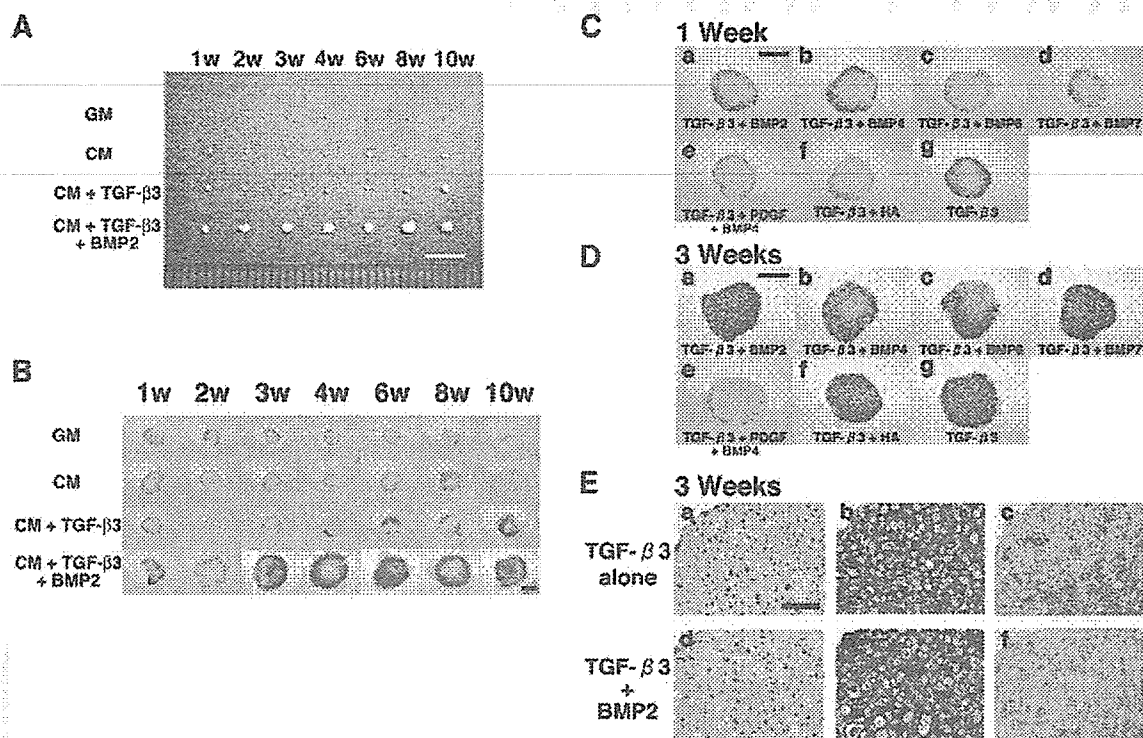
A

B

C 1 Week

D 3 Weeks

E 3 Weeks

COLOR

Fig. 1. In vitro chondrogenesis of KUM5 cells. A,B: Time-course analysis of growth factors-induced matrix production in KUM5 cells. Macroscopic view of KUM5 chondrogenic nodules which were generated after pellet culture for 1–10 weeks in the GM or the CM supplemented with or without growth factors as indicated (see "Cell culture" Section in Materials and Methods) (A) and Toluidine blue stained section (B). BMP2 drastically enhanced TGF-β3-induced matrix production of KUM5 cells.

C,D: Toluidine blue stained section of KUM5 chondrogenic nodules in the pellet culture exposed to growth factors as indicated for 1 week (C) or 3 weeks (D). E: Higher magnification of KUM5 chondrogenic pellet exposed to TGF-β3 (a–c), or TGF-β3 and BMP2 (d–f) for 3 weeks. a,d: Hematoxylin and Eosin stain; b,e: Toluidine blue stain; c,f: Alcian blue stain. Scale bars: 5 mm (A), 500 µm (B, C, D), 100 µm (E).

et al., 1994]. (http://1954.jukuin.keio.ac.jp/ume-zawa/chip/sugiki) by using the Affymetrix gene chip oligonucleotide arrays (Table I). RNAs were isolated from cell lines cultured in the GM without any induction of differentiation to perform the gene chip analysis. Of the 23,000 genes represented on the gene chip, chondro-cyte-specific- or associated-genes such as type II collagen α1, Sox9, and cartilage oligomeric matrix protein were more strongly expressed in KUM5 cells than in other marrow-derived mesenchymal cells. Surprisingly, OP9 cells [Nakano, 1996] also expressed these chondro-cyte-specific or -associated genes at higher levels: the type II collagen α1, and cartilage oligomeric matrix protein genes were expressed in OP9 cells at more than tenfold higher levels than in 9–15c mesenchymal stem cells, KUSA-O osteo-adipogenic progenitor cells, H-1/A pre-adipocytes, or even KUM5 chondroblasts. These results implied that KUM5 and OP9 cells have increased chondrogenic potential.

Pelleted Micromass Culture of OP9 Cells

We performed the pellet culture of OP9 cells in the GM and continued the culture for up to 10 weeks (Fig. 2A). The cells were equally embedded in the extracellular matrix and the extracellular matrix of the OP9 pellet culture did not show metachromasie with the toluidine blue stain in the GM (data not shown). With exposure to TGF-β3, the cells in the peripheral zone generated cartilage and exhibited adipocyte-like morphology in the center (Fig. 2Bg,Cg). Next, we investigated the effect of BMP2 in the pellet culture of OP9 cells. The CM with TGF-β3 and BMP2 dramatically induced the chondrogenic differentiation (Fig. 2A,Ba,Ca), that is, the pellet cells produced abundant extracellular matrix (Fig. 2D) and caused deeper metachromatic staining and an enlarged metachromatic area (Fig. 2Db). Additionally, we examined the effect of other cytokines on the differentiation of OP9 cells

TABLE I. Cartilage-Associated Genes Expressed in KUM5 and OP9 Cells in Comparison With Other Marrow Stromal Cells

Probe set	Genbank	Description	9–15c		KUSA-O		KUSA-A1		H-1/A		OP9		KUM5		Symbol
			Flags	Raw	Flags	Raw	Flags	Raw	Flags	Raw	Flags	Raw	Flags	Raw	
1450567_a_at	NM_031163	Procollagen, type II, alpha 1	A	28	A	187	A	98	A	46	P	1,7390	P	679	Col2a1
1428571_at	AK004383	Procollagen, type IX, alpha 1	P	85	P	116	P	99	P	57	P	132	P	130	Col9a1
1422253_at	NM_009925	Procollagen, type X, alpha 1	A	13	A	20	A	15	A	104	A	218	A	270	Col10a1
1418599_at	BB836814	Procollagen, type XI, alpha 1	A	69	P	682	P	4,284	P	5,009	A	2,551	P	515	Col11a1
1419527_at	NM_016685	Cartilage oligomeric matrix protein	A	120	A	111	A	64	A	167	P	1,892	M	172	Comp
1449368_at	NM_007833	Decorin	A	176	A	36	A	223	A	226	A	85	A	110	Dcn
1416405_at	BC019502	Biglycan	P	12,600	P	11,817	P	11,011	P	12,932	P	21,954	P	18,640	Bgn
1449827_at	NM_007424	Aggrecan 1	A	70	A	118	A	105	A	127	A	94	A	167	Agc1
1416321_s_at	BC019775	Proline arginine-rich end leucine-rich repeat	P	196	A	59	P	899	P	1,092	P	2,169	P	362	Prelp
1415939_at	NM_021355	Fibromodulin	P	388	M	359	P	11,542	P	16,626	A	108	A	320	Fmod
1418745_at	NM_012050	Osteomodulin	P	288	A	50	P	1,849	P	2,185	P	347	P	743	Omd
1415943_at	BC010560	Syndecan 1	P	1,182	P	2,449	P	1,358	P	1,607	P	4,704	P	1,799	Sdc1
1417012_at	AI266824	Syndecan 2	P	752	P	1,256	P	2,940	P	4,398	P	605	P	2,039	Sdc2
1420853_at	NM_011520	Syndecan 3	A	382	A	547	P	680	P	902	P	355	P	762	Sdc3
1417654_at	NM_011521	Syndecan 4	P	306	P	281	P	244	P	342	P	305	P	320	Sdc4
1420950_at	BI077717	SRY-box containing gene 9	P	120	A	5	A	59	A	27	P	183	P	183	Sox9
1420895_at	BM248342	Transforming growth factor, beta receptor I	P	780	P	703	P	657	P	862	P	1,344	P	802	Tgfbr1
1425444_a_at	S69114	Transforming growth factor, beta receptor II	P	552	P	746	P	1,068	P	1,189	P	1,595	P	1,133	Tgfbr2
1425620_at	AF039601	Transforming growth factor, beta receptor III	P	448	A	328	A	275	P	313	P	868	P	1,015	Tgfbr3
1422912_at	NM_007554	Bone morphogenetic protein 4	P	1,048	P	646	P	6,470	P	7,266	P	1,736	P	2,890	Bmp4
1425492_at	BM248248	Bone morphogenetic protein receptor, type 1A	P	1,486	P	815	P	1,089	P	1,164	P	1,159	P	1,123	Bmpr1a
1420847_a_at	NM_010207	Fibroblast growth factor receptor 2	P	833	P	656	P	1,664	P	1,998	P	992	P	3,595	Fgfr2
1417271_a_at	NM_007932	Endoglin	A	247	A	187	A	40	A	115	P	222	P	1,371	Eng
1451314_a_at	L08431	Vascular cell adhesion molecule 1	P	462	A	39	P	28	A	92	A	812	P	583	Vcam1

The raw data from the gene chip analysis are available at our laboratory's web site (http://1954.jukuin.keio.ac.jp/umezawa/chip/sugiki). Flag indicates the presence or absence of gene expression determined by presence/absence call (Affymetrix). P (presence): gene is expressed. M (marginal): gene is marginally expressed. A (absence): gene is not expressed.

COLOR

A

B

C

D
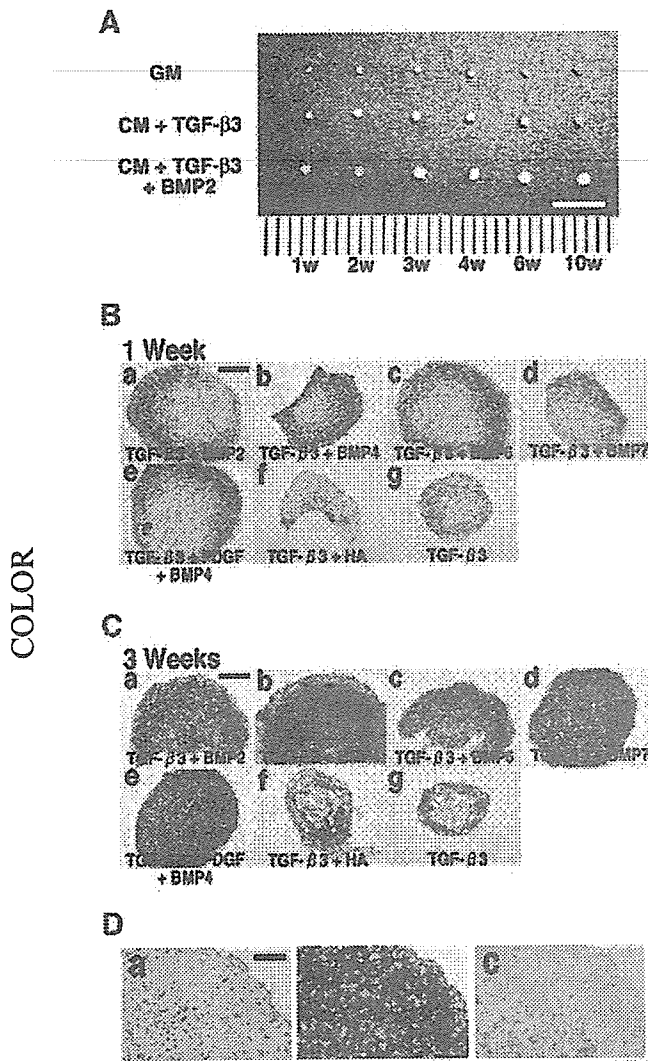

Fig. 2. In vitro chondrogenesis of OP9 cells. A: Time-course analysis of growth factors-induced matrix production in OP9 cells. Macroscopic view of OP9 chondrogenic nodules which were generated after pellet culture for 1–10 weeks in the GM or the CM supplemented with growth factors as indicated. BMP2 drastically enhanced TGF-β3-induced matrix production of OP9 cells. B,C: Microscopic view of OP9 chondrogenic nodules in the pellet culture exposed to growth factors as indicated for 1 week (B) or 3 weeks (C). D: OP9 chondrogenic pellet exposed to TGF-β3 and BMP2 for 3 weeks. a: Hematoxylin and Eosin stain; b: Toluidine blue stain; c: Alcian blue stain. Scale bars: 5 mm (A), 200 μm (B,C), 100 μm (D).

with procedures analogous to those used for KUM5 cells. BMP4, BMP6, and BMP7 enhanced the TGF-β3-induced differentiation in a manner similar to BMP2 (Fig. 2B,C). Unlike its effect in KUM5 cells, PDGF did not inhibit TGF-β3- and BMP4-induced differentiation, as determined by toluidine blue staining (Fig. 2Be,Ce). To confirm the chondrogenetic

differentiation histologically, we examined the ultrastructural analysis of the cartilaginous micromasses. Extracellular matrix was abundantly deposited over OP9 cells, or the surface of the generated micromass (Fig. 3D). The cells covering the micromass showed a flattened shape (Fig. 3E). The OP9 chondrocytes inside the micromass showed an oval or round structure, had cellular processes, and were embedded in the hypertrophic chondrocytes. Abundant rough endoplasmic reticulum and a small number of mitochondria were observed in the OP9 chondrocytes (Fig. 3F).

Cell Surface Markers in KUM5 and OP9 Cells

To characterize the KUM5 and OP9 cells, we analyzed the cell surface markers by using flowcytometry. KUM5 cells were positive (more than tenfold compared to the isotype control) for CD9, CD105 (endoglin), Sca-1 and Ly-6C, marginal for CD106 (VCAM-1) and CD140a (PDGFRα), and negative for c-kit (CD117), Flk-1, CD31 (PECAM-1), CD34, CD144 (VE-cadherin), CD45 (leukocyte common antigen), CD49d (integrin α4), CD90 (Thy-1), CD102, CD14, Ly-6G, and CD41 (Fig. 4A). OP9 cells were strongly positive for CD140a, CD106, and CD9, weakly positive for Sca-1, and negative for CD105, c-kit, Flk-1, CD31, CD34, CD144, CD45, CD49d, CD90, CD102, CD14, Ly-6C, Ly-6G, and CD41 (Fig. 4B). Next, we performed hierarchical clustering by analyzing the global gene expression pattern for cell type classification and cell function prediction. When 244 cell surface marker genes are used for analysis, KUM5 and OP9 formed one cluster independent of seven other marrow stromal cells (Fig. 4C, Supplementary Table I, http://1954.jukuin.-keio.ac.jp/umezawa/sugiki/pca). We then performed PCA to determine whether it is possible to discriminate OP9 and KUM5 from other cells in three-dimensional expression space. Using the same gene sets for clustering analysis, KUM5 and OP9 cells can clearly separated from the other seven cell lines (Fig. 4D). The similarity of the in vitro phenotype of KUM5 and OP9 cells was supported by the results of grouping the marrow stromal cells into subcategories in terms of cell surface markers.

Global Outlook by Hierarchical Clustering and PCA by Fat- and Cartilage-Associated Genes

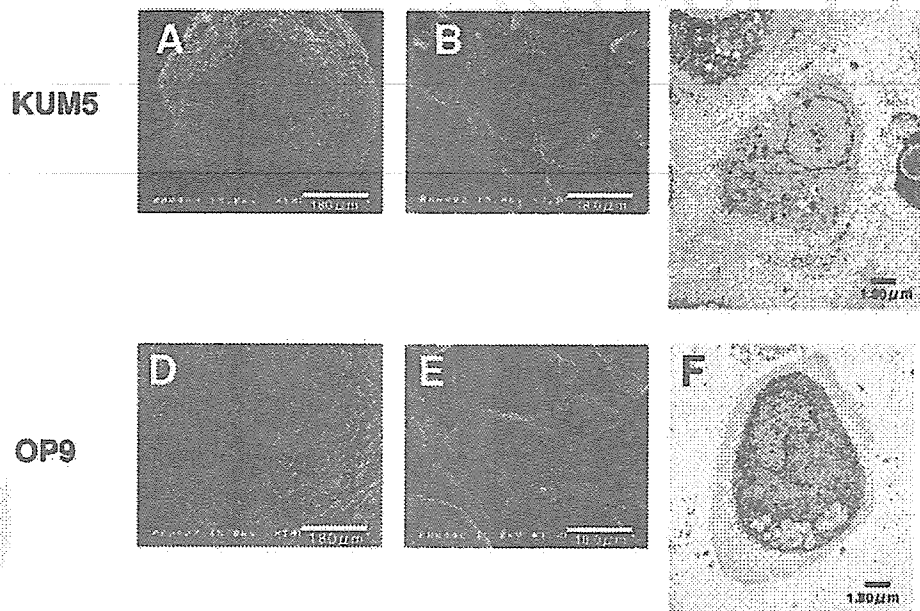We also performed hierarchical clustering and PCA on the expression pattern of fat- and

Fig. 3. Ultrastructural analysis of the in vitro chondrogenic micromass. Micromasses of KUM5 cells (A–C) and OP9 cells (D–F) were generated by culturing in the CM supplemented with TGF-β3 for 3 weeks. (A,B,D,E), SEM; (C,F), TEM.

cartilage-associated genes. Using 34 fat-associated genes (Supplementary Table II), KUM5 and OP9 were separated and show smaller distance by both hierarchical clustering and PCA, implying that the KUM5 and OP9 cells have similar characteristics compared with other seven marrow stromal cells (Fig. 5A–D). In contrast, the analysis of 36 cartilage-associated gene expression data (Fig. 5E, Supplementary Table III) demonstrated that these two cell lines were not grouped into the same subcategory. Both cells showed "P: positive" expression in sox9 and α1(II) procollagen genes, and OP9 cells expressed cartilage-specific and - associated genes such as the α1(II) procollagen, α1(XI) procollagen, cartilage oligomeric matrix proteins, and proline arginine-rich end leucine-rich repeat genes at higher levels, when compared to KUM5 cells (Table I). These results imply that OP9 cells are differentiated chondrocytes as a default state while KUM5 cells are oligopotent mesenchymal cells that have a tendency to differentiate into chondrocytes.

In Vivo Chondrogenesis

To examine the chondrogenic activity of KUM5 cells, we injected KUM5 cells at confluence without any treatment (i.e., without TGF-β3 and BMP2 treatment) into mice sub-cutaneously (Fig. 6A). KUM5 cells generated cartilage-like structures within 1 week and complete cartilage at 3 weeks, and the generated cartilage exhibited metachromasia with toluidine blue staining. Interestingly, the cartilage generated by KUM5 cells showed enchondral ossification at 4 weeks. We then implanted the KUM5 chondrogenic micromass after pellet culture into the subcutaneous tissue just beneath the cutaneous muscle (Fig. 6B). The KUM5 cartilage was formed within 1 week and it exhibited typical chondrogenic structures: post-mitotic daughter cells in the cell nest, hypertrophic chondrocytes, and abundant metachromatic matrix with toluidine blue staining. The immunohistochemical analysis showed that KUM5 cartilage stained positive for chondrocyte-specific type II collagen (Fig. 6C), while only a slight amount of type II collagen was detected in the in vitro pelleted micromass culture. Ultrastructural analysis revealed that KUM5 chondrocytes implanted into the subcutaneous tissue of nude mice were embedded in the lacunae cavities and had abundant endoplasmic reticulum and a small number of mitochondria (Fig. 6D), and collagen fibers were produced around the lacunae cavity of the KUM5 chondrocytes, as is the case of the in vitro conditions (Fig. 6E).
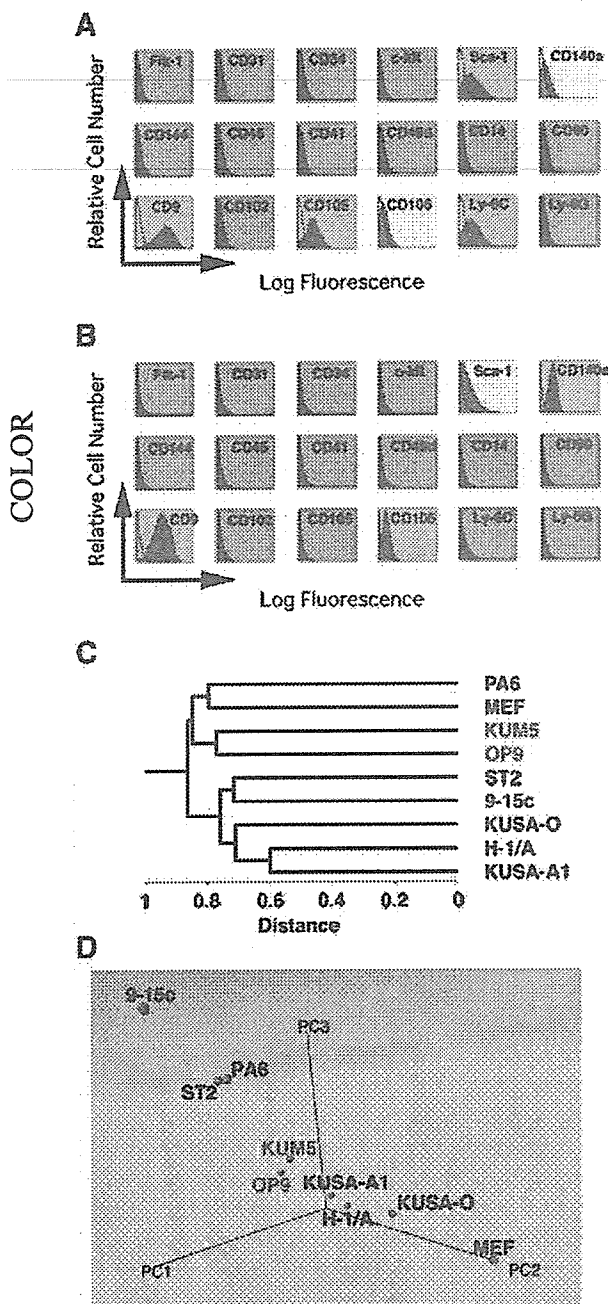
Fig. 4. Expression profiling, hierarchical clustering, and principal component analysis (PCA) of cell surface markers in marrow stromal cells. **A,B:** Flow cytometric analysis of cell surface markers in KUM5 cells (A) and OP9 cells (B). Red and pink colors indicate positive and marginal expression, respectively, and blue color indicates negative expression. **C:** Dendrogram revealing clustering profile of nine marrow stromal cells using 244 surface marker genes (Supplementary Table I). **D:** The rotated and dimensionally reduced gene expression data. Nine marrow stromal cells are plotted onto the 1st, 2nd, and 3rd principal component using 244 surface marker genes. These results indicate that KUM5 and OP9 cells were grouped into the same subcategory.
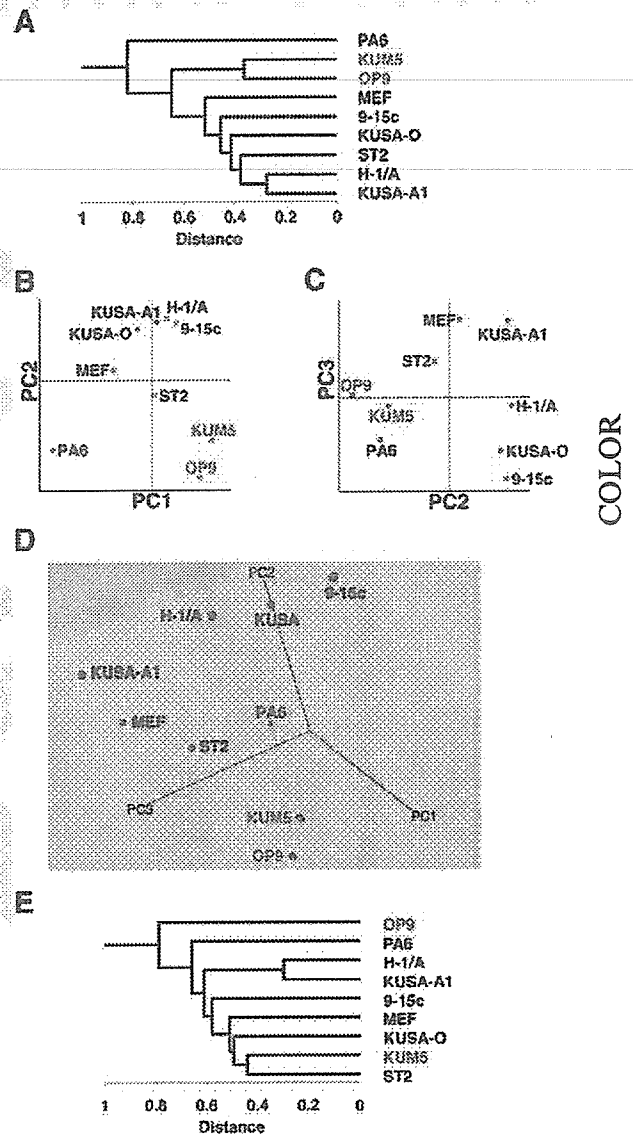
Fig. 5. Hierarchical clustering and PCA of fat- and cartilage-associated gene expression in marrow stromal cells. A. Dendrogram revealing clustering profile of 9 marrow stromal cells using 34 fat-associated genes (Supplementary Table II). B–D. PCA on expression levels of 34 fat-associated genes. The gene expression data from 9 marrow stromal cells were analyzed. Nine marrow stromal cells are plotted onto 2D-representation, PC1 and PC2 axes (B) or PC2 and PC3 axes (C), and 3D-representation (D). These results indicate that KUM5 and OP9 cells were grouped into the same subcategory. E. Dendrogram revealing clustering profile of 9 marrow stromal cells using 36 cartilage-associated genes (Supplementary Table III).

To determine the chondrogenic activity of OP9 cells in vivo, we directly injected them into the subcutaneous tissue. The OP9 cells without any induction did not generate cartilage. We then implanted the OP9 chondrogenic
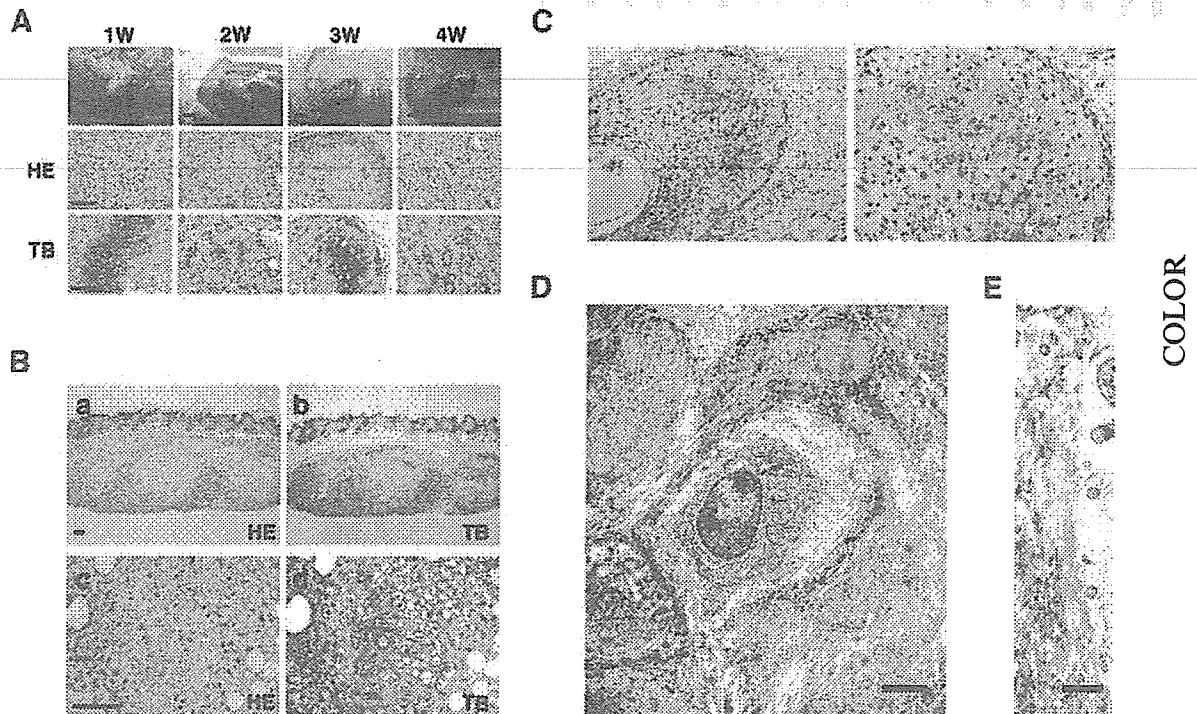
Fig. 6. In vivo chondrogenesis of KUM5 cells. A: Macroscopic view (top), hematoxylin and eosin stain (HE) (middle) and toluidine blue stain (TB) (bottom) analysis at 1, 2, 3, and 4 week (w)-cultivation in vivo after direct injection of KUM5 cells. B: KUM5 chondrogenic nodules, that were generated after pellet culture for 7 days in the CM supplemented with TGF-β3 and BMP2, were implanted just beneath the cutaneous muscle in the subcutaneous tissue and were cultivated in vivo for 3 weeks. Panels c and d are higher magnifications of a and b, respectively.

C: Expression of chondrocyte-specific collagen type II. The KUM5 chondrogenic nodules were sectioned after 2 week-in vivo cultivation and stained with collagen type II-specific antibody. D,E: Ultrastructural analysis (TEM) of KUM5 implants. KUM5 cells were implanted into the subcutaneous tissue of Balb/c nu/nu mice, and the generated cartilage was resected 2 weeks after implantation. Scale bars: 2 mm (A, top row), 100 μm (A, middle and bottom row), 100 μm (B), 2 μm (D), 1 μm (E).

micromass after the pellet culture into the subcutaneous tissue just beneath the cutaneous muscle (Fig. 7A,B). The OP9 cartilage was formed at 2 and 4 weeks, and abundant metachromatic matrix was observed with the toluidine blue stain. The immunohistochemical analysis shows that OP9 cartilage stains positive for the chondrocyte-specific type II collagen (Fig. 7C).

Sorting of Chondroblasts by Chondrocyte-Specific Cis-Regulatory Element of the Collagen α2(XI) Gene

Although the KUM5 cells used in this study were derived from a single-cell origin or clone, it could be argued that both cells responsive and non-responsive to chondrogenic induction were present [Ko et al., 1990]. In this sense, KUM5 cells might have been a largely heterogeneous cell population. Even cells derived from a single clone have been shown to be heterogeneous in

terms of differentiation capacity and stages [Muraglia et al., 2000]. To validate the chondrogenic differentiation observed here, a homogenous population of committed cell obtained after induction should be isolated. Therefore, for the purpose of sorting chondrogenically committed cells, we transfected KUM5 cells with a Venus-expression vector under the control of the Col α2(XI) promoter, analyzed the transfected cells, and collected Venus-positive cells (Fig. 8A–D). The sorted cells were assessed for in vitro (Fig. 9A–F) and in vivo chondrogenesis (Fig. 9G–I). The cells again showed metachromatic chondrogenic micromasses with toluidine blue staining in vitro (Fig. 9B). Direct injection of the cells resulted in the cartilage formation within 1 week and obvious enchondral ossification at the periphery of the cartilage at 4 weeks (Fig. 9G). Again, ultrastructural analysis revealed that KUM5 chondrocytes implanted into the subcutaneous
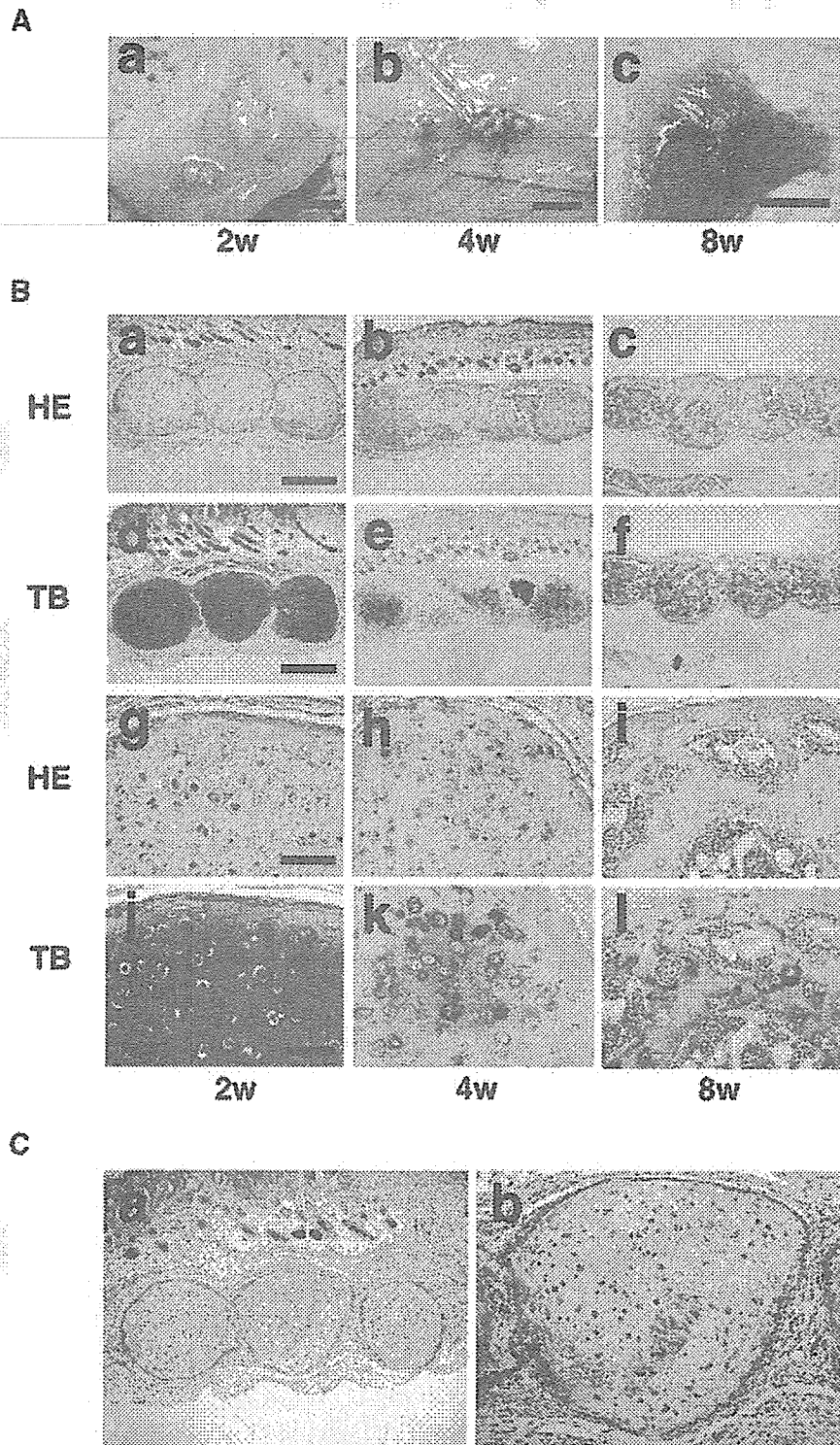
Fig. 7. In vivo chondrogenesis of OP9 cells. In vivo chondrogenesis was examined by implantation of OP9 chondrogenic nodules. OP9 chondrogenic nodules, which were generated after pellet culture for 7 days in the CM supplemented with TGF-β3 and BMP2, were implanted just beneath the cutaneous muscle in the subcutaneous tissue and were cultivated in vivo for the number of weeks indicated. **A:** Macroscopic view of OP9 cartilage after 2 (a), 4 (b), and 8 (c)-week-in vivo cultivation.

B: Histological analysis of OP9 cartilage after 2 (a,d,g,j), 4 (b,e,h,k), and 8 (c,f,i,l)-week-in vivo cultivation. (a,b,c,g,h,i), HE stain; (d,e,f,j,k,l), TB stain. **Panels g–l** are higher magnifications of a–f, respectively. **C:** Immunohistochemical analysis of the in vivo OP9 chondrogenic nodules. The OP9 chondrogenic nodules after 2-week-in vivo cultivation stained positive for collagen type II. Scale bars: 2 mm (A), 500 μm (Ba–f), 100 μm (Bg–l).
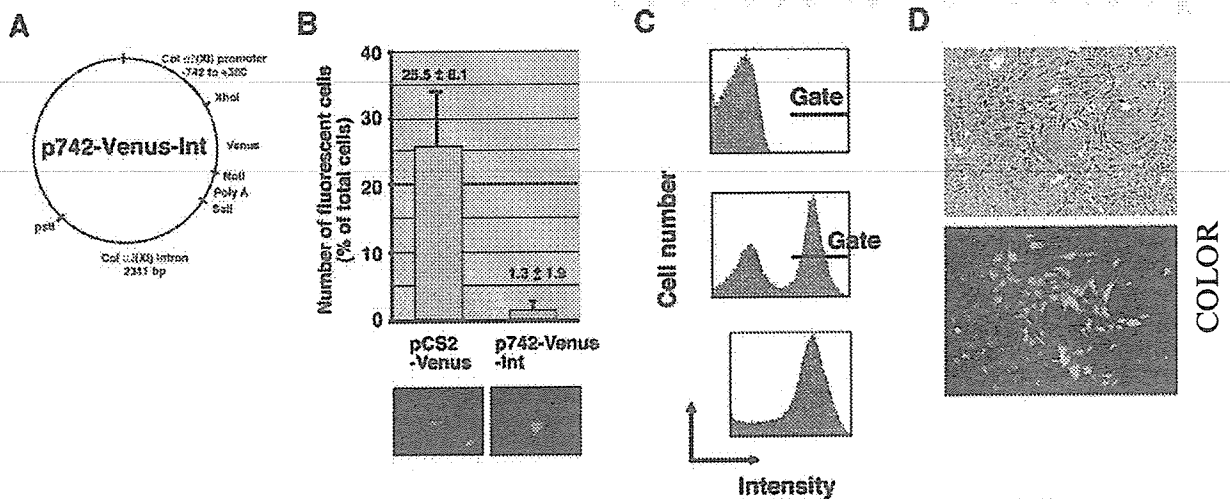
Fig. 8. Isolation of KUM5 chondroblasts using the chondroblast-specific cis-regulatory element. **A:** The p742-Venus-Int plasmid containing the fluorescent Venus gene driven by the cis-regulatory elements of the α2(XI) collagen gene. **B:** The number of fluorescent KUM5 cells (upper) after transfection with the p742-Venus-Int plasmid or pCS2-Venus containing the Venus gene driven by the CMV-promoter. Fluorescent photomicrograph of KUM5 cells after the first sorting (lower). **C:** Flowcytometric analysis of KUM5 cells after transfection with the p742-Venus-Int plasmid (top); The fluorescence-positive cells were sorted, propagated, and analyzed (middle). Again, the propagated fluorescence-positive cells were sorted, propagated, and analyzed (bottom). The "gate" for sorting is shown by the horizontal bar in the upper and middle panels. More than 80% of cells became positive after the final sorting. **D:** Phase contrast micrograph (upper) and fluorescent photomicrograph (lower) of the finally sorted cells (the lower panel of C).

tissue of nude mice were embedded in the hypertrophic chondrocytes and had abundant endoplasmic reticulum and a small number of mitochondria (Fig. 9H,I). The post-mitotic daughter cells in the cell nest, which are often observed in cartilage, were also detected (Fig. 9I).

DISCUSSION

In this study, we focus on the chondrogenic differentiation in vitro and in vivo using the two cell lines, KUM5 and OP9. The chondrogenic process is determined by the sequential expression of matrix component, and the differential response of differentiating cells to the growth factors may be attributed to the differentiating stages that depend on the expression patterns of the gene set as is the case for hematopoietic cells. The process of the chondrogenic differentiation is influenced by a number of growth factors including TGF-β and/or BMPs. Three isoforms of TGF-β have been known to have the ability to induce the chondrogenic differentiation. Both TGF-β2 and -β3 are more effective than TGF-β1 in promoting chondrogenesis, and TGF-β3 accelerates production of cartilaginous extracellular matrix in differentiating mesenchymal stem cells [Barry et al., 2001].

This study was undertaken to obtain mesenchymal stem cells with chondrogenic potential that retain critical in vivo cell functions, as do mammary gland epithelial cells, skin keratinocytes, and pigmented epithelial cells. To achieve this, we attempted to identify marrow-derived cells with chondrogenic nature and immortality without transformation among the cells obtained by the limiting-dilution method [Umezawa et al., 1992], defining "immortality" simply as indefinite cell division.

OP9 cells are known to serve as a niche or a specific microenvironment for the regulation of self-renewal and differentiation of stem cells [Nakano, 1996], and the question is raised of whether marrow stromal cells or marrow-derived mesenchymal cells with chondrogenic potential are capable of constituting a microenvironment for stem cells. It is inconceivable that cartilage can form a niche for cells in the living body based on structural and morphological considerations; however, a cell with chondrogenic or adipo-chondrogenic potential may serve as a niche not only in the case of OP9 cells but also as a general concept, at least in vitro.
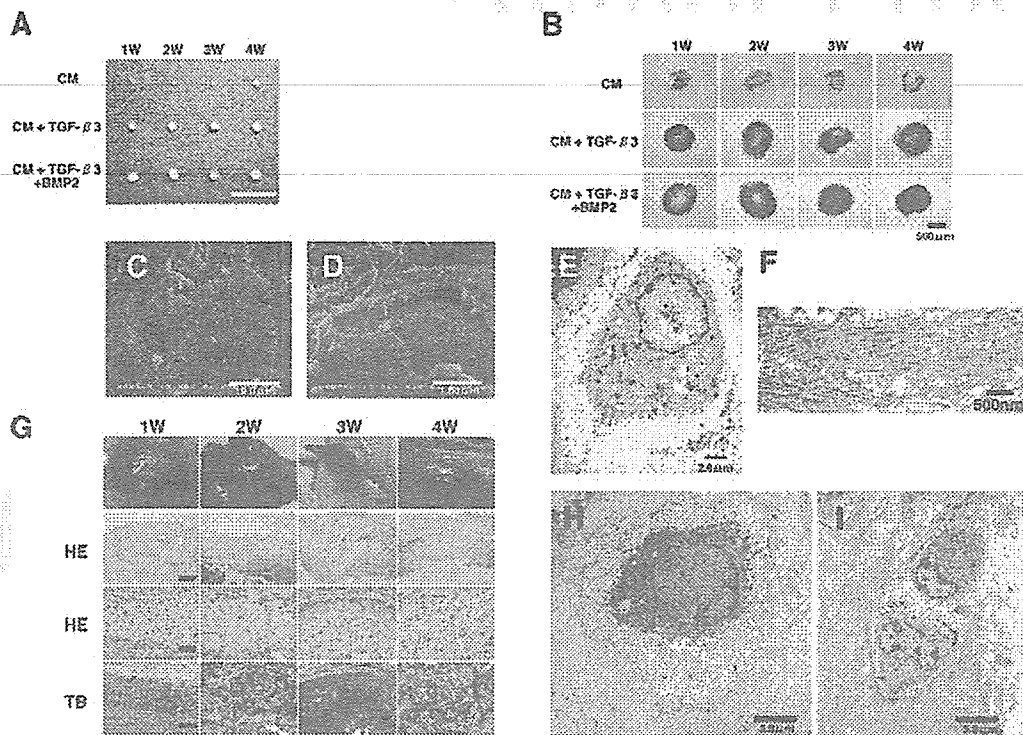
Fig. 9. In vitro and in vivo chondrogenesis of KUM5 cells sorted according to the activity of the chondrocyte-specific cis-regulatory element. A,B: Macroscopic view of the chondrogenic nodules which were generated after pellet culture of the finally sorted KUM5 cells for 1–4 weeks in the CM supplemented with growth factors as indicated (A) and toluidine blue stained section (B). C–F: Ultrastructural analysis of the micromasses of KUM5 cells sorted according to the activity of the Col α2(XI) cis-regulatory element (KUM5-Venus) after culturing in the CM supplemented with TGF-β3 for 3 weeks. (C,D), SEM; (E,F), TEM. G: In vivo chondrogenesis was examined 1–4 weeks after direct injection of the finally sorted KUM5 cells. From top to bottom: Macroscopic view, scale bars: 2 mm; histological analysis, scale bar: 600 μm, HE stain; histological analysis, scale bar: 120 μm, HE stain; histological analysis, scale bar: 120 μm, TB stain. H,I: Ultrastructural analysis (TEM) of the sorted KUM5 cartilage. The sorted KUM5 cells were implanted into the subcutaneous tissue of Balb/c nu/nu mice, and the generated cartilage was resected 2 weeks after implantation. Scale bars: 5 mm (A), 500 μm (B), 2 mm (G, top row), 500 μm (G, 2nd row), 100 μm (G, 3rd and bottom row).

The sequence of enchondral or perichondral ossification by KUM5 and OP9 cells was as follows: deposition of homogeneous matrix surrounding the small nests of the injected cells that subsequently became positive for type II collagen and exhibited metachromasia with toluidine blue staining, trapping them in the secreted homogeneous matrix, and the appearance of small nests of isogenous chondrocytes that probably resulted from repeated cell division. At a later stage, that is, 4–8 weeks after injection, the peripheral region of the generated cartilage became ossified. Importantly, the chondrogenesis by KUM5 and OP9 cells was irreversible and reproducible, and the implanted cells never transformed into malignant cells, formed any abnormal extracellular matrices, or induced any significant inflammatory reactions. It is again noteworthy that the osteogenesis by these two different lines of cells was mediated by chondrogenesis, and it was therefore considered to be chondral ossification. Thus, the unique characteristics of these two cell lines provide an opportunity to analyze the process of enchondral or perichondral ossification in an experimental system in detail.

In fetal life, primary ossification centers form by one of two processes: enchondral ossification or membranous ossification. Enchondral ossification refers to bony replacement of cartilage and is the mode of formation of the long bones. During membranous ossification mesenchymal cells form membranes within which ossification occurs and this is the mode of formation of the scapula and skull and, in part, of the clavicle and pelvis. After birth, bone growth continues by both enchondral and membranous ossification. Further enchondral ossification occurs in